research articles Journal of proteome research

Combined NMR and LC−DAD-MS Analysis Reveals Comprehensive Metabonomic Variations for Three Phenotypic Cultivars of *Salvia Miltiorrhiza* Bunge

Hui Dai,[†,‡] Chaoni Xiao,[†,‡,§] Hongbing Liu,[†,‡] Fuhua Hao,[†] and Huiru Tang*[,†]

State Key Laboratory of Magnetic Resonance and Atomic and Molecular Physics, Wuhan Centre for Magnetic Resonance, Wuhan Institute of Physics and Mathematics, Chinese Academy of Sciences, Wuhan 430071, P.R.China, College of Life Sciences, Northwest University, Xi'an 710069, P.R. China, and Graduate University of the Chinese Academy of Sciences, Beijing 100049, P.R. China

Received November 14, 2009

Metabonomic analysis is an important molecular phenotyping method for understanding plant ecotypic variations and gene functions. Here, we systematically characterized the metabonomic variations associated with three *Salvia miltiorrhiza* Bunge (SMB) cultivars using the combined NMR and LC−DAD-MS detections in conjunction with multivariate data analysis. Our results indicated that NMR methods were effective to quantitatively detect the abundant plant metabolites including both the primary and secondary metabolites whereas the LC−DAD-MS methods were excellent for selectively detecting the secondary metabolites. We found that the SMB metabonome was dominated by 28 primary metabolites including sugars, amino acids, and carboxylic acids and 4 polyphenolic secondary metabolites, among which *N*-acetylglutamate, asparate, fumurate, and yunnaneic acid D were reported for the first time in this plant. We also found that three SMB cultivars growing at the same location had significant metabonomic differences in terms of metabolisms of carbohydrates, amino acids, and choline, TCA cycle, and the shikimate-mediated secondary metabolisms. We further found that the same SMB cultivar growing at different locations differed in their metabonome. These results provided important information on the ecotypic dependence of SMB metabonome on the growing environment and demonstrated that the combination of NMR and LC−MS methods was effective for plant metabonomic phenotype analysis.

Keywords: *Salvia miltiorrhiza* Bunge (SMB) • NMR • LC−DAD-MS • ecotype • PCA (principal component analysis) • OPLS-DA (orthogonal projection to latent structure with discriminant analysis)

Introduction

Molecular phenotyping is an important approach for plant functional genomic studies especially when only subtle or no obvious phenotypic variations are observable in the morphological level.[1−3] In such cases, analysis of plant metabolite composition (metabonome) and its variations associated with the phenotypes becomes a particularly useful systems biological approach for phenotypic characterization in the molecular level. This is because metabonomics concerns with the metabonome of the integrated biological systems and dynamic responses to the alteration of endogenous and/or exogenous factors.[4,5] In fact, metabonomics approaches have already been established as a powerful tool for understanding the molecular aspects of gene functions,[1,6] mammalian pathophysiology,[7−9] epidemiology,[10−12] toxicity,[13,14] environmental sciences[15,16] and plant physiology.[17,18] Such applications have also been extended to metabolic phenotyping of potato,[19,20] *Arabidopsis thaliana*,[21] chamomile flowers[22] and green tea.[23] Technically, metabonomic analysis demands comprehensive and complete determination of all metabolites in the concerned biological fluids and/or tissues followed with linking the metabonomic variations induced by the aforementioned factors with the underlying biological events. For plant molecular phenotypings which require effective analysis for both primary and secondary metabolites, however, many challenges remain for metabonomic analytical methods due to the complexity of plant metabolite composition and limitations of a single analytical method.

Currently, NMR spectroscopy and chromatography−mass spectrometry (LC−MS and GC−MS) are two major methods for detecting and quantifying plant metabolite compositions.[24−26] NMR techniques are intrinsically reproducible with rich structure information and spectral signal intensities are directly proportional to analyte concentration since all analytes in a mixture (e.g., metabonome) have the same response coefficients.[4,5,26] Such methods are advantageous to quantitatively measure all abundant primary and secondary metabolites of plants in a single spectrum.[26] In contrast, the LC−MS

* To whom correspondence should be addressed. E-mail: huiru.tang@wipm.ac.cn. Telephone: +86-(0)27-87198430. Fax: +86-(0)27-87199291.
† Wuhan Institute of Physics and Mathematics, Chinese Academy of Sciences.
‡ Graduate University of the Chinese Academy of Sciences.
§ Northwest University.

10.1021/pr901045c

Published on Web 01/13/2010

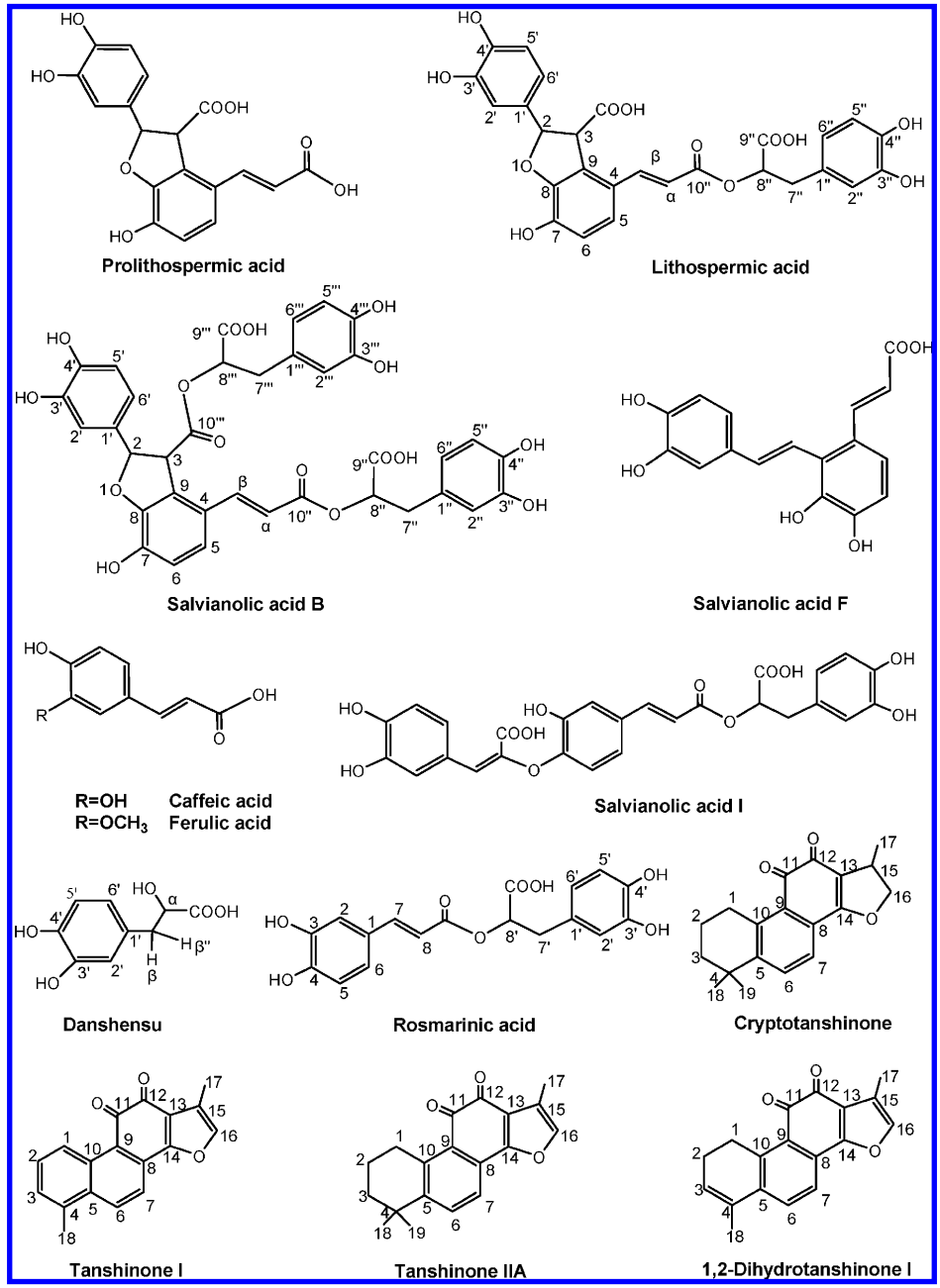

Figure 1. Structures of some typical secondary metabolites of SMB.

methods are metabolite-selective and sensitive for the targeted analysis enabling detection of low-concentration compounds which may not be detectable with NMR. Markedly different LC−MS response coefficients for different metabolites,[27] on the other hand, demand *in situ* calibration curves for metabolite quantification. It is therefore apparent that the combination of these methods offers the combined advantages although only limited such studies have reported so far.[26,27]

Salvia miltiorrhiza Bunge (SMB) represents an excellent challenging example for effective plant molecular phenotypings with complex metabonome, which is well-defined in terms of both primary and secondary metabolite structures.[27−29] This plant also has important medicinal applications in treatments of cardiovascular[30] and liver diseases[31] due to antioxidant activities[32,33] of its secondary metabolites such as polyphenolic acids and tanshinones, some of which are shown in Figure 1. Furthermore, there are three SMB cultivars, namely, *Salvia miltiorrhiza* Bunge cv. *Sativa* (SA), cv. *Foliolum* (SF) and cv. *Silcestris* (SI), which differ in productivity, disease resistance and commodity yields.[34] These cultivars were used either as mixtures or as replacement to each other in medicinal practice although their metabolite compositional equivalence was not thoroughly assessed. Even for the authentic SMB, cultivation at different geographic locations may result in different metabolic phenotypes since the plant metabolite compositions vary with the growing conditions.[22,35] Detailed metabolic phenotyping (metabotyping) is particularly relevant in this case since the SMB metabolite compositions are important for its bioactivity, quality and consistency assurance. In fact, a previous LC−DAD study has already reported some differences for SMB cultivars[36] and the same cultivar grown at different locations.[37] However, this study only considered some selected SMB secondary metabolites and the holistic metabonomic differences remain to be assessed for these SMB ecotypes.

In this work, we have systematically analyzed the metabolite compositions of three SMB cultivars and a cultivar obtained from four different growing locations using the combined NMR and LC−DAD-MS methods. The objectives are to (1) assess the effectiveness of combined NMR and LC−DAD-MS methods in plant (metabolic) molecular phenotyping and (2) define the statistically significant metabonomic features associated with three different SMB ecotypes and the same cultivar from different growing locations.

Materials and Methods

Chemicals. Methanol, formic acid, $K_2HPO_4 \cdot 2H_2O$ and $NaH_2PO_4 \cdot 12H_2O$ were purchased from Guoyao Chemical Co. Ltd. (Shanghai, China) all in analytical grade. HPLC-grade acetonitrile was obtained from J.T. Baker Pharmaceuticals Company (Phillipsburg, NJ). Water used for HPLC was purified by a Milli-Q system (Millipore, Milford, MA). D_2O (99.9% D) and sodium 3-trimethlysilyl [2,2,3,3-d_4] propionate (TSP) were purchased from Cambridge Isotope Laboratories Inc. (Andover, MA). Phosphate buffer (K_2HPO_4−NaH_2PO_4, 0.1 M, pH = 7.4), containing 10% D_2O and TSP (0.2 mM), was prepared in H_2O.

Materials and Sample Preparation. The fresh SMB roots of three cultivars, namely, *Salvia miltiorrhiza* Bunge cv. *Sativa* (SA), *Salvia miltiorrhiza* Bunge cv. *Foliolum (SF), Salvia miltiorrhiza* Bunge cv. *Silcestris* (SI), were purchased in October 2006 from the same cultivation base at Zhongjiang county in Sichuan province, southwest China. The fresh roots of *Salvia miltiorrhiza* Bunge cv. *sativa* were also obtained from four cultivation bases in October 2006 at different geographic locations, namely, Zhongjiang in Sichuan (A), Wuhan in Hubei (B), Anding in Hebei (C), and Nanyang in Henan (D). The plant materials were all air-dried at ambient with good ventilation for 2−3 days and then sealed in separate plastic bags followed with storage in a brown desiccator to prevent from moisture and light exposure.

All dried SMB materials were ground with a coffee blender and sieved through a 2 mm sieve. In all cases, the same pool of raw materials from 10−15 individual plants was divided into five portions and each portion (about 1 g) was extracted with 15 mL of 50% aqueous methanol by intermittent sonication (i.e., 1 min sonication with 1 min break) at ambient with the sonication bath temperature strictly controlled under 25 °C. The supernatants were collected by 10 min centrifugation (10000 rpm with a benchtop centrifuge) and the remaining solid residues were further extracted twice using the same procedure. The combined supernatant from three extractions was condensed at 30 °C with a rotary evaporator to remove the organic solvents followed with lyophilization. To ensure the suitability and validity of above sampling methods for the purposes of this study, we also compared the metabolite composition of extracts from above methods with those from five independent pools of plants (each contained raw materials from two individual plants). No significant differences were found between them.

NMR Measurements. The extracts (about 2 mg) were dissolved into 600 μL of phosphate buffer (0.1 M, pH7.4) containing 10% D_2O (v/v) and TSP (0.2 mM) in 5 mm NMR tubes, respectively. All ^{1}H NMR spectra were recorded at 298K on a Bruker AV III 600 MHz NMR spectrometer equipped with an inverse detection cryogenic probe. ^{1}H NMR spectra were acquired using standard one-dimensional pulse sequence (recycle delay-90°-t_1-90°-t_m-90°-acquisition) and water suppression was achieved with a weak continuous wave irradiation during both the recycle delay (RD, 2 s) and mixing time, t_m, of 100 ms. t_1 was set to 4 μs and 90° pulse length was adjusted to about 10 μs. Sixty-four transients were collected into 32k data points for each spectrum with a spectral width of 20 ppm and an acquisition time of 1.36 s. All free induction decays (FIDs) were multiplied by an exponential function with a 0.3 Hz line broadening factor prior to Fourier transformation (FT).

For quantitation purposes, spin−lattice relaxation time (T_1) was measured using the classical "inversion recovery" sequence [RD-180°-τ-90°-acquisition] with water suppressed during both recycle delay (RD) and relaxation delay τ. Sixteen τ values were employed (0.1−14.5 s) with the total repetition time of 21.4 s (i.e., RD plus acquisition time) and 32 scans were acquired with 32k points.

For resonance assignment purposes, ^{1}H−^{1}H COSY, ^{1}H−^{1}H TOCSY, ^{1}H *J*-resolved, ^{1}H−^{13}C HSQC and ^{1}H−^{13}C HMBC 2D NMR spectra were acquired on selected samples. In both COSY and TOCSY experiments, 48 transients were collected into 2048 (2k) data points for each of 128 increments with spectral widths of 6313 Hz in both dimensions. The MLEV-17 was employed as spin-lock scheme for TOCSY with the mixing time of 80 ms. In *J*-resolved spectra, 32 transients were collected into 2k data points for each of 50 increments with spectral width of 6313 and 50 Hz in F_2 (chemical shift) and F_1 (J coupling constant) dimensions respectively. ^{1}H−^{13}C HSQC and HMBC 2D NMR spectra were recorded using the gradient selected sequences with the direct ^{1}H−^{13}C J-coupling constant of 145 Hz. In HSQC experiments, composite pulse broadband ^{13}C decoupling (globally alternating optimized rectangular pulses, GARP) was also employed during the acquisition period; 240 transients were collected into 2k data points for each of 128 increments with spectral width of 6313 Hz in ^{1}H and 26410 Hz in the ^{13}C dimension. In HMBC experiments, 400 transients were collected into 2k data points for each of 128 increments with spectral width of 6313 Hz in ^{1}H and 33201 Hz in the ^{13}C dimension; the long-range coupling constant was set to 6 Hz. These data were zero-filled to 2k data points in the evolution dimension and appropriate apodization functions were applied to the FID prior to FT with forward complex linear prediction.

Quantification of Metabolites. In an incompletely relaxed NMR spectra obtained in our experiments, the integral area for a given proton resonance obeys the following equation (eq 1):

$$A^m = A_0^m[1 - \exp(-t/T_1^m)] \quad (1)$$

where t is total relaxation time (i.e., RD plus acquisition time); A_0^m and A^m are the integral areas for the signals of a given proton m (with spin−lattice relaxation time of T_1^m) in the completely relaxed state and a given spectrum, respectively. The signal integrals for proton m and internal reference TSP in a given spectrum have following relationship (eq 2)

$$\frac{A_0^m}{A_0^{TSP}} = \frac{A^m}{A^{TSP}} * \frac{1 - \exp(-t/T_1^{TSP})}{1 - \exp(-t/T_1^m)} \quad (2)$$

where A_0^{TSP} and A^{TSP} are the integrals for methyl groups of TSP in the completely relaxed and a given spectrum, respectively; T_1^{TSP} is the spin−lattice relaxation time for methyl protons of TSP. The concentration of a metabolite (C_m) and TSP (C_{TSP}) in the same spectra obeys the relationship described in eq 3 taking

into consideration of proton numbers related to the NMR signals (eq 3),

$$C_m = \frac{N_{\mathrm{TSP}} C_{\mathrm{TSP}}}{N_m} * \frac{A_0^m}{A_0^{TSP}} = \frac{N_{\mathrm{TSP}} C_{\mathrm{TSP}}}{N_m} * \frac{A^m}{A^{\mathrm{TSP}}} * \frac{1 - \exp(-t/T_1^{\mathrm{TSP}})}{1 - \exp(-t/T_1^m)} \quad (3)$$

where N_m and N_{TSP} denote proton numbers for the corresponding metabolite signal and the methyl groups of TSP (i.e., 9 protons), respectively. Using eq 3, the concentration of a given metabolite can be calculated with the known concentration of TSP. The errors for metabolite quantity measured with the NMR methods here were estimated to be well below 15% using standard salvianolic acid B solutions (0.3597 and 1.4406 mM).

HPLC−DAD-ESI−MS Measurements. LC−MS analysis of the aforementioned extracts was performed on an Agilent 1200 system (Agilent Technologies, Waldbronn, Germany) equipped with a quaternary solvent delivery system, an online degasser, an autoampler, a column temperature controller, a diode-array detector (DAD) and a Bruker microQTOF mass spectrometer (Bruker Daltonics, Germany) with an electrospray ionization source operating in either positive ion or negative ion mode. An ACE C18-HL column (5 μm, 250× 4.6 mm) with C18 guard column was used at 30 °C with the injection volume of 10 μL (5 mg/mL). The monitoring wavelength was set to 280 nm with the acquisition wavelength for the DAD set to about 210−600 nm. The mobile phases consisted of water (A) and acetonitrile (B) both containing 0.1% (v/v) formic acid in a stepped gradient mode as follows: 0−0.5 min, 5% B; 0.5−40 min, 5 to 37% B; 40−50 min, 37 to 60% B; 50−55 min, 60 to 74% B; 55−68 min, 74 to 80% B; 68−75 min, 80 to 83% B. The flow rate was 1 mL/min with five percent of the eluent directed to MS using a BNMI unit (Bruker BioSpin). The mass spectrometry parameters were as follows: nebulizer gas pressure, 0.8 bar; drying gas flow rate, 8 L/min; gas temperature, 180 °C; capillary voltage, 4500 V and −4000 V for negative and positive ion mode respectively. For full-scan MS analysis, the spectra were recorded in the range of m/z 50−1000.

Data Treatments and Multivariate Analysis. Baseline and phase corrections for the NMR spectra were manually achieved using TOPSPIN (v2.0, Bruker Biospin) with all spectra referenced to TSP at δ0.0 ppm. The spectral region δ0.5−10.0 was segmented into regions of 0.004 ppm width (2.4 Hz) using the AMIX package (v3.8.3, Bruker Biospin) with the regions δ4.70−4.95 and δ3.34−3.39 discarded to eliminate the effects of imperfect water suppression and residual methanol signal. All remaining spectral segments were scaled to the total integrated area of the spectrum to reduce variations resulting from the concentration inconsistency before multivariate statistical analyses. Principal components analysis (PCA) and orthogonal projection to latent structure with discriminant analysis (OPLS-DA)[38] were performed with the SIMICA-P$^+$ software (v11.0, Umetrics, Sweden). The results are visualized in the forms of the scores plots, where each point represents an individual sample's metabonome, and loadings plots in which each data point represents an NMR spectral region contributing to group clustering. PCA was carried out with mean-centered data and OPLS-DA was done with unit variance scaling (UV). In the latter, one orthogonal and one predictive component were calculated using the NMR data as *X*-matrix and the class information as *Y*-matrix with 5-fold cross validation. The quality of the model was described by the cross-validation parameter Q^2, indicating the predictability of the model, and R^2X, which represents the total explained variables for the *X* matrix. The back-transformed loadings of OPLS-DA were color-coded with the square of coefficients (r^2) to indicate the significances of the variables (or metabolites) contributing to classification using MATLAB scripts (http://www.mathworks.com/) with some in-house modifications. The hot colored (e.g., red) variables contribute more significantly to the classification than the cold colored (e.g., blue) ones. In this study, the coefficient cutoff value of 0.81 ($r < -0.81$ or $r > 0.81$) was employed based on the discrimination significance at the level of $p < 0.05$ according to the test for the significance of the Pearson product-moment correlation coefficients. The absolute concentration for some metabolites was also obtained from well resolved signals and subjected to the classical statistical analysis (one way-ANOVA).

For the LC−UV and LC−MS data, multivariate data analysis was conducted with the same software on the integral areas of 12−27 major signals including polyphenolic acids such as danshensu, salvianolic acid H/I, rosmarinic acid, lithospermic acid, salvianolic acid B, salvianolic acid L and tanshinones such as 15,16-dihydrotanshinone I, 1,2-dihydrotanshinone I, tanshinone I, trijuganone B, cryptotanshinone, and tanshinone IIA normalized to the weights of extracts assuming that the response coefficients for the same metabolite was not drastically different in different samples. For LC−UV data, the integrals of the chromatographic peaks at a fixed UV wavelength (280 nm) were used for statistical analysis. For LC−MS data, the peak integrals from the base peak chromatograms obtained from the MS instrument software were employed for statistical analysis. PCA and OPLS-DA were conducted with the loadings and coefficients calculated in the same fashion as described above.

Results and Discussion

^{1}H NMR and HPLC−DAD-MS Analysis of SMB Extracts. Figures 2 and 3 show some representative ^{1}H NMR spectra of SMB extracts from *Salvia miltiorrhiza* Bunge cv. *Sativa* grown at Zhongjiang (A), Wuhan (B), Anding (C) and Nanyang (D) (Figure 2) and from three different ecotypes (Figure 3). The resonance assignments were achieved based on the literature data[39–41] and the atomic connectivity obtained from a catalogue of two-dimensional NMR spectra including ^{1}H−^{1}H COSY, ^{1}H−^{1}H TOCSY, ^{1}H−^{1}H *J*-resolved, ^{1}H−^{13}C HSQC and ^{1}H−^{13}C HMBC 2D NMR. The assigned resonances were tabulated in Table 1 together with the corresponding ^{1}H, ^{13}C NMR chemical shifts and signal multiplicities. The results showed that the SMB metabonome was dominated by 4 polyphenolic acids (secondary metabolites), including salvianolic acid B, lithospermic acid, rosmarinic acid and danshensu (see structures in Figure 1), and 28 primary metabolites including 5 sugars, 8 carboxylic acids, 10 amino acids and choline, which is similar to our previous findings.[27] However, N-acetylglutamate, aspartate and fumarate were detected for the first time in this plant.

We also measured the spin−lattice relaxation time (T_1) values for metabolite resonances with good resolutions (Table 2). The same metabolites in different samples have similar T_1 values which are smaller than 2s for most metabolites. On the basis of these values, we further calculated the absolute concentration of selected metabolites (in the forms of mg/g extracts) from five parallel samples (Tables 3 and 4). The abundant primary metabolites include raffinose (316−427 mg/g), sucrose (10−80 mg/g), malate (10−24 mg/g) and glutamine (5−45 mg/g)

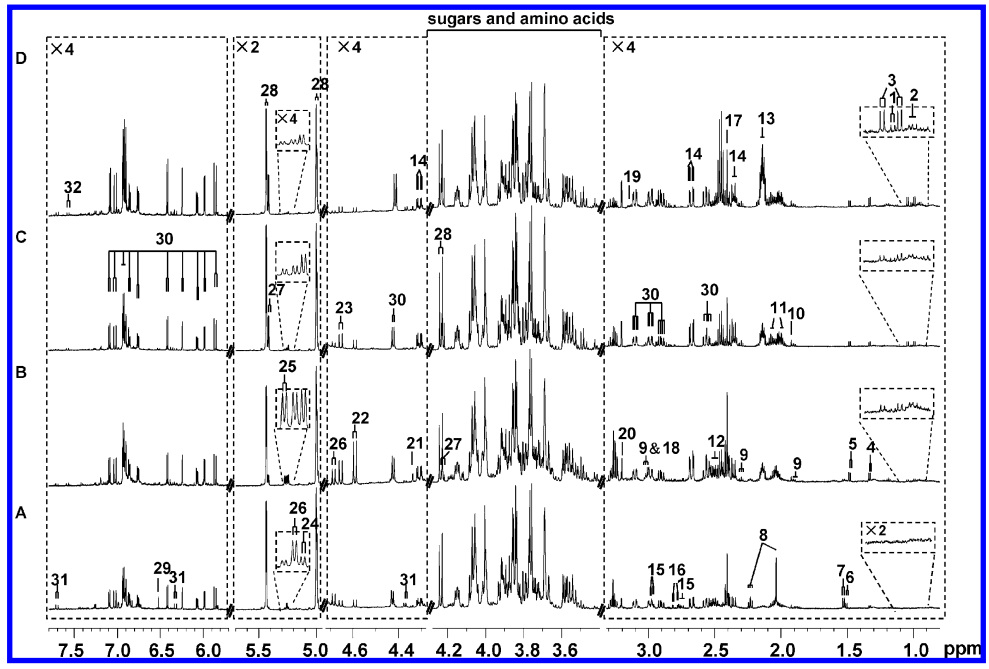

Figure 2. [1]H NMR spectra (600 MHz) of SMB extracts from four different geographic locations, namely, Zhongjiang, Sichuan (A), Wuhan, Hubei (B), Anding, Hebei (C), and Nanyang, Henan (D). The spectral regions δ3.32−0.80, δ4.72−4.28, δ5.70−4.95 were vertically expanded for 4, 4, and 2 times, respectively, whereas the region δ7.80−5.70 was expanded for 4 times (see Table 1 for metabolite identification key).

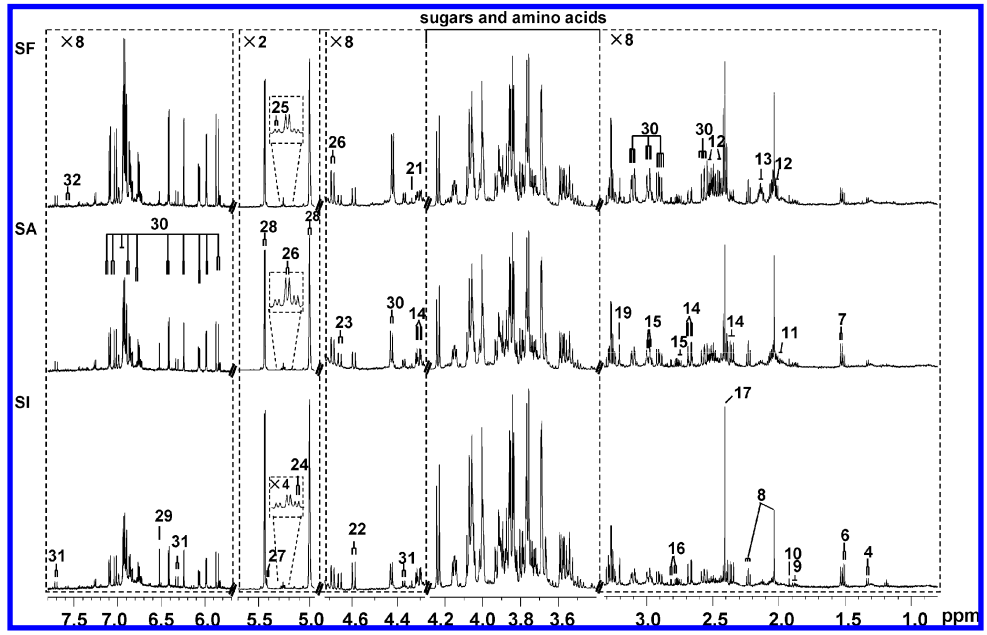

Figure 3. [1]H NMR spectra (600 MHz) of SMB extract from *Salvia miltiorrhiza* Bunge cv. *Sativa* (SA), cv. *Foliolum* (SF) and cv. *Silcestris* (SI). The spectral regions δ3.22−0.88, δ4.72−4.28 and δ5.70−4.95 were vertically expanded for 8, 8, and 2 times, respectively, whereas the region δ7.80−5.70 was expanded for 8 times (see Table 1 for metabolite identification key).

whereas the abundant SMB secondary metabolites include salvianolic acid B (68−134 mg/g), lithospermic acid (4−10 mg/g), danshensu (about 6 mg/g) and rosmarinic acid (3−5 mg/g).

Only secondary metabolites were detected in LC−UV (Figure S1 and S2, Supporting Information) and LC−MS (Figure S3 and S4, Supporting Information) profiles including 12 polyphenolic acids, 12 tanshinones, 4 steroids and 2 others together with 10 unknown minor compounds. Most of their identities were tentatively assigned here according to literatures[42] using pseudomolecular and fragment ions together with UV absorbance (see Table S1 for details, Supporting Information). Generally, the polyphenolic acids showed their quasi-molecular ions (i.e., $[M - H]^-$ and $[2M - H]^-$) in the negative ion mode whereas both polyphenolic acids and diterpenoids exhibited their quasi-molecular ions (i.e., $[M + H]^+$ and $[M + Na]^+$) in the positive ion mode. A minor metabolite (peak 40 in Figure S3b, Supporting Information) detected for the first time in SMB showed a parent ion $[M - H]^-$ at m/z 539 and a fragment ion at m/z 341 (a loss of 198) in the negative ion MS mode, indicating its molecular mass of 540 Da and the presence of a danshensu

Table 1. NMR Assignments of the Abundant SMB Metabolites

peak no.	metabolites	assignment	δ^1H (multiplicity[a])	δ^{13}C	assigned with
1	Isoleucine	δ-CH_3	0.94	14.1	TOCSY, JRES, HSQC
		γ-CH_3	1.01	17.5	
		γ'-CH	1.47	27.1	
		β-CH	1.97	38.8	
2	Leucine	δ-CH_3	0.96	23.6	TOCSY, JRES, HSQC
		β-CH_2	1.72	42.8	
3	Valine	γ'-CH_3	0.99 (d, 6.9 Hz)	19.6	TOCSY, JRES, HSQC
		γ-CH_3	1.04 (d, 6.9 Hz)	20.9	
		β-CH	2.26	31.9	
4	Lactate	β-CH_3	1.34 (d, 7.0 Hz)	22.2	TOCSY, JRES, HSQC, HMBC
		α-CH	4.13	69.6	
		COOH		185.3	
5	Alanine	β-CH_3	1.49 (d, 7.4 Hz)	18.0	TOCSY, JRES, HSQC, HMBC
		α-CH	3.79	53.5	
		COOH		178.9	
6	U_1	CH_3	1.51 (d, 7.1 Hz)	18.1	TOCSY, JRES, HSQC, HMBC
			3.71	59.9	
		COOH		178.0	
7	U_2	CH_3	1.53 (d, 7.3 Hz)	18.1	TOCSY, JRES, HSQC, HMBC
			3.77	59.6	
		COOH		178.1	
8	*N*-Acetylglutamate	-CH_2	1.90	29.4	TOCSY, JRES, HSQC, HMBC
		-$COCH_3$	2.04	31.0	
		γ-CH_2	2.23 (t, 7.9 Hz)	32.1	
		α-CH	4.12	57.8	
		C═O		176.5	
		COOH		184.0	
9	γ-aminobutyrate	β-CH_2	1.90	26.7	TOCSY, JRES, HSQC, HMBC
		α-CH_2	2.30 (t, 7.5 Hz)	37.2	
		γ-CH_2	3.01 (t, 7.3 Hz)	42.5	
		COOH		184.5	
10	Acetate	CH_3	1.93 (s)	26.1	JRE, HSQC, HMBC
		COOH		184.2	
11	Proline	γ-CH_2	2.00 (m)	26.5	TOCSY, JRES, HSQC, HMBC
		δ'-CH	3.34 (m), 3.42 (m)	49.2	
		β-CH_2	2.34 (m)	31.7	
		α-CH	4.14 (m)	64.1	
		COOH		177.6	
12	Pyroglutamate	γ'-CH	2.04	28.7	TOCSY, HSQC, HMBC
		β-CH_2	2.43	32.5	
		γ-CH	2.51	28.7	
		α-CH	4.18	61.6	
		C═O		185.1	
		COOH		182.5	
13	Glutamine	β-CH_2	2.15 (m)	29.6	TOCSY, JRES, HSQC, HMBC
		γ-CH_2	2.45 (m)	33.7	
		α-CH	3.79	57.0	
		COOH		176.8, 181.0	
14	Malate	β'-CH	2.37	45.9	TOCSY, JRE, HSQC, HMBC
		β-CH	2.68 (dd, 15.6, 3.5 Hz)	45.9	
		α-CH	4.31	73.7	
		COOH		176.3	
15	Danshensu	β-CH	2.76 (dd, 7.8, 14.1 Hz)	39.3	TOCSY, JRE, HSQC, HMBC
		β''-CH	2.98 (dd, 4.3, 14.1 Hz)	39.3	
		α-CH	4.17 (dd, 4.3, 7.8 Hz)	76.0	
		6′-CH	6.73 (dd, 2, 8 Hz)	124.6	
		2′-CH	6.83 (d, 2 Hz)	120.7	
		5′-CH	6.86 (d, 8 Hz)	119.6	
		COOH		183.4	
16	Aspartate	β-CH	2.76	60.8	TOCSY, JRE, HSQC, HMBC
		β'-CH	2.82 (dd, 5.6, 16.8 Hz)	38.7	
		α-CH	3.87	[b]	
		COOH		176.2, 180.2	
17	Succinate	CH_2	2.42 (s)	35.8	JRE, HSQC, HMBC
		COOH		184.5	
18	α-Ketoglutaric acid	β-CH_2	2.45	33.7	TOCSY, JRE, HSQC
		γ-CH_2	3.01 (t, 7.3 Hz)	38.9	

Table 1 Continued

peak no.	metabolites	assignment	δ^1H (multiplicity[a])	δ^{13}C	assigned with
19	Malonate	CH_2	3.13 (s)	[b]	JRE, HMBC
		COOH		180.2	
20	Choline	$N(CH_3)^+$	3.21 (s)	54.9	JRE, HSQC, HMBC
		CH_2		68.4	
21	Tartaric acid	CHOH	4.34 (s)	79.1	JRE, HSQC, HMBC
		COOH		181.7	
22	β-Galactose	C_1H	4.59 (d, 7.8 Hz)	99.6	TOCSY, JRE, HSQC, HMBC
		C_2H	3.50	74.7	
		C_3H	3.66	76.0	
		C_4H	3.94	72.1	
23	β-Glucose	C_1H	4.65 (d, 7.8 Hz)	99.2	TOCSY, JRE, HSQC, HMBC
		C_2H	3.26	76.8	
		C_3H	3.48	74.2	
24	α-Glucose	C_1H	5.24 (d, 3.9 Hz)	95.5	TOCSY, JRE, HSQC, HMBC
		C_2H	3.55	72.5	
		C_3H	3.72	69.4	
		C_4H	3.42	72.1	
		C_5H	3.85	71.9	
25	α-Galactose	C_1H	5.27 (d, 3.9 Hz)	95.5	TOCSY, JRE, HSQC, HMBC
		C_2H	3.83	65.2	
		C_5H	4.02	72.8	
26	Melibiose	Glc-αC_1H	5.26 (d, 3.8 Hz)	95.5	TOCSY, JRE, HSQC, HMBC
		Glc-αC_2H	3.55	72.3	
		Glc-αC_3H	3.72	75.9	
		Glc-αC_5H	4.03	73.0	
		Glc-βC_1H	4.69 (d, 8.0 Hz)	99.0	
		Glc-βC_2H	3.28	77.1	
		Glc-βC_3H	3.50	74.7	
		Glc-βC_4H	3.65	76.2	
27	Sucrose	Glc-C_1H	5.42 (d, 3.8 Hz)	95.5	TOCSY, JRE, HSQC, HMBC
		Glc-C_2H	3.57	73.7	
		Glc-C_3H	3.81	75.6	
28	Raffinose	Glc-C_1H	5.44 (d, 3.9 Hz)	95.1	TOCSY, JRE, HSQC, HMBC
		Glc-C_2H	3.57	72.7	
		Glc-C_3H	3.77	70.6	
		Glc-C_5H	4.07	74.0	
29	Fumarate	CH=CH	6.52 (s)	138.0	JRE, HSQC, HMBC
		COOH		177.4	
30	Salvianolic acid B[c]	7″-H	2.90 (dd, 14.4, 9.7 Hz)	39.8	TOCSY, JRE, HSQC, HMBC
		7″-H	3.10 (dd, 14.4, 3.9 Hz)	39.8	
		8″-H	5.00 (dd, 9.7, 3.9 Hz)	79.5	
		α-CH=CH	5.87 (d, 16.0 Hz)	118.5	
		β-CH=CH	6.99 (d, 16.0 Hz)	144.7	
		7‴-H	2.98	39.2	
		7‴-H	2.56	39.2	
		8‴-H	4.90	80.6	
		2-H	5.98 (d, 5.6 Hz)	89.5	
		3-H	4.33 (d, 5.6 Hz)	59.5	
		2‴-H	6.24 (d, 2.6 Hz)	119.7	
		5‴-H	6.42 (d, 8.0 Hz)	119.2	
		6‴-H	6.08 (dd, 8.0, 2.6 Hz)	123.2	
		6″-H	6.76	124.3	
		5″-H	6.93	115.8	
		5-H	7.06 (d, 8.0 Hz)	125.7	
		6-H	6.92	119.3	
31	Lithospermic acid	α-CH=CH	6.32 (d, 16.0 Hz)	[b]	TOCSY, JRE
		β-CH=CH	7.70 (d, 16.0 Hz)	[b]	
32	Rosmarinic acid	8-CH=CH	6.34 (d, 16.0 Hz)	[b]	TOCSY, JRE
		7-CH=CH	7.58 (d, 16.0 Hz)	[b]	

[a] Multiplicity: singlet (s), doublet (d), triplet (t), doublet of doublets (dd), multiplet (m) U: unidentified signal. [b] The signals or the multiplicities were not determined. [c] See Figure 1 for atom labeling.

residue. On the basis of the literature data, its identity was tentatively assigned to yunnaneic acid D which was found previously in *Salvia yunnanensis*.[43]

These results indicated that NMR and LC−MS methods obtained different but complementary metabolite information. While NMR detected the abundant metabolites including

Table 2. T_1 Values for the Proton Signals of Some Selected Metabolites (Unit: s)[a]

		different geographic locations				different ecotypes		
	δ(ppm)	A	B	C	D	SA	SI	SF
TSP	0	3.20 ± 0.03	3.07 ± 0.03	3.16 ± 0.08	3.15 ± 0.02	3.20 ± 0.03	3.05 ± 0.03	3.47 ± 0.01
Isoleucine	1.01 (d)	–[b]	–[b]	–[b]	1.00 ± 0.09	–[b]	–[b]	–[b]
Valine	1.04 (d)	0.99 ± 0.02	1.10 ± 0.10	1.07 ± 0.05	1.05 ± 0.05	–[b]	–[b]	–[b]
Lactate	1.33 (d)	1.30 ± 0.15	1.24 ± 0.13	1.33 ± 0.11	1.12 ± 0.06	–[b]	–[b]	–[b]
Alanine	1.48 (d)	–[b]	1.80 ± 0.20	1.76 ± 0.10	1.45 ± 0.07	–[b]	–[b]	–[b]
N-Acetylglutamate	2.23 (t)	0.89 ± 0.18	–[b]	–[b]	–[b]	0.89 ± 0.18	0.76 ± 0.11	1.04 ± 0.20
Glutamine	2.14 (m)	1.04 ± 0.09	1.12 ± 0.18	1.16 ± 0.03	1.10 ± 0.02	1.04 ± 0.09	1.07 ± 0.18	1.11 ± 0.20
Succinate	2.41 (s)	2.17 ± 0.06	2.41 ± 0.02	2.44 ± 0.06	2.38 ± 0.02	2.17 ± 0.06	2.30 ± 0.04	2.53 ± 0.08
Malate	2.68 (dd)	1.02 ± 0.20	1.01 ± 0.05	1.35 ± 0.05	1.20 ± 0.08	1.02 ± 0.20	1.18 ± 0.10	1.19 ± 0.22
Sucrose	5.41 (d)	1.03 ± 0.08	1.06 ± 0.16	0.92 ± 0.10	0.97 ± 0.10	1.03 ± 0.08	0.96 ± 0.02	1.04 ± 0.07
Raffinose	5.43 (d)	0.87 ± 0.07	0.84 ± 0.06	0.92 ± 0.04	0.90 ± 0.04	0.87 ± 0.07	0.93 ± 0.03	0.86 ± 0.10
Salvianolic acid B	7.03 (d)	1.80 ± 0.20	1.37 ± 0.08	1.66 ± 0.12	1.69 ± 0.07	1.80 ± 0.20	1.87 ± 0.09	1.60 ± 0.17

[a] A, B, C and D denote SMB extracts obtained from Zhongjiang, Sichuan; Wuhan, Hubei; Anding, Hebei; and Nanyang, Henan. SA, SI and SF mean SMB extracts obtained from *Salvia miltiorrhiz* Bunge cv. *Sativa* (SA), cv. *Foliolum* (SF) and cv. *Silcestris* (SI). Standard deviations refer to the error on T_1 fitting. [b] T_1 was not determined due to weakness or overlapping of signals.

Table 3. Coefficients from OPLS-DA and Metabolite Contents in SMB Extracts from Four Different Geographic Locations[a]

	coefficient[b]			man ± SD[c] (mg/g)			
metabolite	B/A	B/C	C/D	A	B	C	D
Isoleucine	−0.635	0.720	0.998	0.37 ± 0.06	0.43 ± 0.03	0.45 ± 0.02[f]	0.95 ± 0.02
leucine	−0.943	−0.944	0.996	–	–	–	–
Valine	−0.792	0.779	0.997	0.46 ± 0.04	0.53 ± 0.03	0.59 ± 0.03[f]	1.35 ± 0.03
Lactate	−0.976	−0.981	0.992	0.48 ± 0.02[d]	0.88 ± 0.02[e]	0.50 ± 0.03[f]	0.95 ± 0.02
Alanine	−0.997	−0.994	0.991	0.36 ± 0.05[d]	1.01 ± 0.03[e]	0.58 ± 0.02[f]	0.84 ± 0.02
Proline	0.807	0.996	0.980	–	–	–	–
N-Acetylglutamate	0.995	−0.998	–	5.28 ± 0.38[d]	3.04 ± 0.38[e]		
Glutamine	−0.998	0.944	0.995	4.86 ± 0.31[d]	15.31 ± 0.50[e]	17.94 ± 1.55[f]	45.23 ± 1.45
Succinate	−0.992	−0.999	0.977	2.07 ± 0.08[d]	3.54 ± 0.16[e]	1.54 ± 0.10[f]	2.04 ± 0.05
Pyroglutamate	−0.904	−0.999	0.994	–	–	–	–
Malate	−0.993	−0.989	−0.993	9.79 ± 0.68[d]	23.99 ± 0.66[e]	17.96 ± 0.87[f]	14.83 ± 0.52
α-Ketoglutaric acid	−0.997	−0.998	0.989	–	–	–	–
Choline	−0.970	0.132	0.910	–	–	–	–
Glucose	−0.990	−0.964	−0.464	–	–	–	–
Melibiose	0.173	−0.984	−0.297	–	–	–	–
Galactose	−0.992	−0.954	−0.297	–	–	–	–
Sucrose	−0.969	0.994	0.936	9.98 ± 2.46[d]	22.22 ± 2.31[e]	72.37 ± 5.38[f]	80.25 ± 1.87
Raffinose	0.990	0.989	−0.844	360.20 ± 16.42[d]	316.03 ± 12.57[e]	426.63 ± 23.65[f]	338.71 ± 15.44
Salvianolic acid B	−0.989	−0.766	0.992	68.07 ± 1.77[d]	85.96 ± 4.06	83.68 ± 3.13[f]	134.23 ± 9.37
Lithospermic acid	0.971	−0.818	0.958	9.26 ± 0.77[d]	5.07 ± 0.50[e]	4.12 ± 0.14[f]	9.49 ± 0.40
Danshensu	0.951	–	–	6.29 ± 0.74[d]	–	–	–
Aspartate	0.895	–	–	–	–	–	–
Rosmarinic acid	−0.822	0.882	0.917	2.80 ± 0.37[d]	3.76 ± 0.09[e]	4.41 ± 0.25[f]	5.18 ± 0.47

[a] A, B, C and D denote SMB extracts obtained from Zhongjiang, Sichuan; Wuhan, Hubei; Anding, Hebei; and Nanyang, Henan. [b] The coefficients from OPLS-DA results, positive and negative signs indicate positive and negative correlation in the concentrations, respectively. The coefficient of 0.81 was used as the cutoff value for the significant difference evaluation ($p < 0.05$). – The absolute concentration was not determined due to signal weakness or overlapping. [c] The absolute concentration and standard deviation (Mean ± SD, mg/g the SMB extracts) were obtained from five parallel samples. [d] Significant difference by one-way ANOVA analysis ($p < 0.05$) A vs B. [e] Significant difference by one-way ANOVA analysis ($p < 0.05$) B vs C. [f] Significant difference by one-way ANOVA analysis ($p < 0.05$) C vs D.

primary metabolites and polyphenolic acids, LC−DAD-MS results showed exclusively secondary metabolites. As observed previously,[27] correlations between signal intensities and concentrations of metabolites are not always available for LC−DAD-MS results probably due to different UV and MS response coefficients for different compounds. In general, polyphenolic acids have good MS responses in both positive and negative ion modes whereas diterpenoids (tanshinones) only have good responses in the positive mode (Figure S3 and S4, Supporting Information). For LC−MS results, the relative metabolite peak intensities in both positive and negative modes are also remarkably different probably due to different ionization efficiency for different compounds.[27] For example, although the molar ratio for rosmarinic acid and salvianolic acid B was about 1:12 in Zhongjiang sample (Table 3), its LC−UV and LC−MS profiles (Figure S1 and Figure S3a, A, Supporting Information) showed that the peak-area ratios (PAR) for these metabolites were about 1:20 and 1:30, respectively. Furthermore, the molar ratio for cryptotanshinone and salvianolic acid B was below 1:32 in the same sample. However, the LC−MS profile (in positive mode) (Figure S3a, A, Supporting Information) showed their PAR as 1:3 whereas the LC−MS profile in the negative ion mode (Figure S3b, A, Supporting Information) failed to detect cryptotanshinone probably due to poor ionization efficiency of this compound in this mode.

Nevertheless, LC−DAD-MS methods are clearly effective in detecting many minor secondary metabolites which are not detectable in NMR offering important complementary infor-

Table 4. Coefficients from OPLS-DA and Metabolite Contents in SMB Extracts from *Salvia miltiorrhiza* Bunge cv. *Sativa* (SA), cv. *Foliolum* (SF) and cv. *Silcestris* (SI)

	coefficient[a]			mean ± SD[b] (mg/g)		
metabolite	SA/SF	SA/SI	SF/SI	SA	SF	SI
Proline	−0.940	−0.981	−0.998	–	–	–
N-Acetylglutamate	−0.703	−0.979	−0.995	5.28 ± 0.38[c]	4.94 ± 0.31	4.00 ± 0.19[e]
Glutamine	0.991	−0.933	−0.995	4.65 ± 0.30[c]	9.21 ± 0.60[d]	4.00 ± 0.19[e]
Succinate	0.997	−0.986	−0.998	2.22 ± 0.15[c]	2.47 ± 0.04[d]	2.02 ± 0.12[e]
Pyroglutamate	0.971	−0.983	−0.997	–	–	–
Malate	−0.945	−0.943	0.939	8.96 ± 0.64[c]	6.62 ± 0.50[d]	8.01 ± 0.46[e]
Choline	0.560	0.425	−0.334	–	–	–
Glucose	−0.705	0.266	0.764	–	–	–
Melibiose	0.886	−0.540	−0.960	–	–	–
Galactose	0.307	0.555	0.540	–	–	–
Sucrose	0.659	0.960	0.954	7.49 ± 1.74[c]	9.11 ± 0.10	18.01 ± 1.89[e]
Raffinose	−0.662	0.980	0.992	362.07 ± 16.00[c]	351.41 ± 6.83	495.55 ± 35.52[e]
Salvianolic acid B	0.976	−0.979	−0.995	66.99 ± 2.37[c]	95.01 ± 7.25[d]	58.79 ± 2.85[e]
Lithospermic acid	0.792	−0.954	−0.994	10.35 ± 0.90[c]	10.41 ± 0.73	8.07 ± 0.46[e]
Danshensu	0.010	−0.420	−0.733	7.17 ± 0.84	7.46 ± 0.74	7.11 ± 0.31
Aspartate	−0.425	−0.601	−0.551	–	–	–
Rosmarinic acid	−0.719	−0.760	−0.738	3.22 ± 0.38	2.85 ± 0.31	2.82 ± 0.25

[a] The coefficients from OPLS-DA results, positive and negative signs indicate positive and negative correlation in the concentrations, respectively. The coefficient of 0.81 was used as the cutoff value for the significant difference evaluation ($p < 0.05$). [b] The absolute concentration and standard deviation (Mean ± SD, mg/g the SMB extracts) were obtained from five parallel samples. − The absolute concentration was not determined due to signal weakness or overlapping. [c] Significant difference by one-way ANOVA analysis ($p < 0.05$) SA vs SI. [d] Significant difference by one-way ANOVA analysis ($p < 0.05$) SA vs SF. [e] Significant difference by one-way ANOVA analysis ($p < 0.05$) SI vs SF.

mation. It is thus obvious that the combination of NMR and LC−DAD-MS data will provide a more holistic way for characterizing plant phenotypic differences in molecular level. The lack of signal-concentration correlation in LC−DAD-MS results is well-known and indicates that careful considerations are necessary for data normalization in LC−MS based metabonomics studies.

Moreover, visual inspections revealed clear differences for SMB samples from different locations and between three ecotypes in both NMR (Figures 2 and 3) and LC−MS spectra (Figure S3 and S4, Supporting Information). For example, the levels of danshensu, fumarate and N-acetylglutamate were much higher in the Zhongjiang (A) samples than in others (Figure 2). The apparent level differences are also observable for glutamine, raffinose and malate in samples from different locations (Figure 2). LC−DAD-MS data further showed marked level differences in a number of secondary metabolites including lithospermic acid, rosmarinic acid and salvianolic acid B resulting from growing locations (Figure S1 and S3, Supporting Information) and cultivars (Figure S2 and S4, Supporting Information). To detect all differences and determine the significances of such differences, multivariate data analysis approaches were employed.

Metabonomic Variations of *S. miltiorrhiza* Bunge cv. *Sativa* from Different Grown Locations. The PCA scores plots (Figure 4) from both NMR and LC−DAD data showed clear classification for the SMB samples grown from four different locations with the first two PCs (PC1 and PC2) explaining more than 90% of variables suggesting the marked metabonomic differences for these samples. Tight intragroup clustering for each group indicates the overall good method reproducibility. The pairwise comparative OPLS-DA of NMR data further showed significant intergroup metabonomic differences with good model quality (Figure 5, left) indicated by the values of R^2X and Q^2. The corresponding loadings plots revealed that the metabolites (Figure 5, right) having significant contributions to the intergroup differences (Table 3) included mainly amino

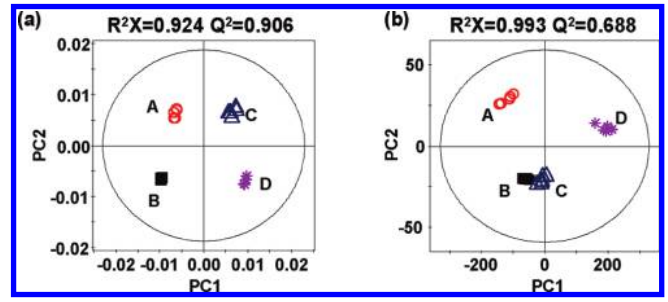

Figure 4. PCA scores plots derived from (a) NMR and (b) LC−UV (280 nm) data for extracts obtained from four different geographic locations: A, Zhongjiang, Sichuan (○); B, Wuhan, Hubei (■); C, Anding, Hebei (Δ); and D, Nanyang, Henan (*)

acids, organic acids, sugars and polyphenolic acids. Compared with the Zhongjiang samples (A), the Wuhan SMB (B) contained more choline, some amino acids (e.g., leucine, alanine and glutamine), sugars (e.g., glucose and sucrose), glycolysis products (e.g., lactate, malate and α-ketoglutarate), salvianolic acid B and rosmarinic acid but less proline, aspartate, N-acetylglutamate, raffinose, lithospermic acid and danshensu. Wuhan SMB samples also contained more sugars (e.g., glucose and melibiose), glycolysis products (e.g., lactate, malate and α-ketoglutarate), some amino acids (e.g., leucine, alanine and pyroglutamate) and lithospermic acid but less proline, glutamine, raffinose, sucrose and rosmarinic acid than Anding samples (C). Furthermore, Anding samples (C) contained more malate and raffinose than Nanyang samples (D) together with less sucrose, choline, amino acids (e.g., leucine, proline and glutamine), glycolysis products such as lactate and α-ketoglutarate, and polyphenolic acids (e.g., rosmarinic acid and salvianolic acid B). This is broadly consistent with the statistical analysis results from the metabolite concentrations.

Similar observations were previously obtained for other plants grown at different locations such as chamomile,[22] olive oils,[44] green tea[23] and *Arabidopsis thaliana* ecotypes[21] probably resulting from some environmental factors such as climate,

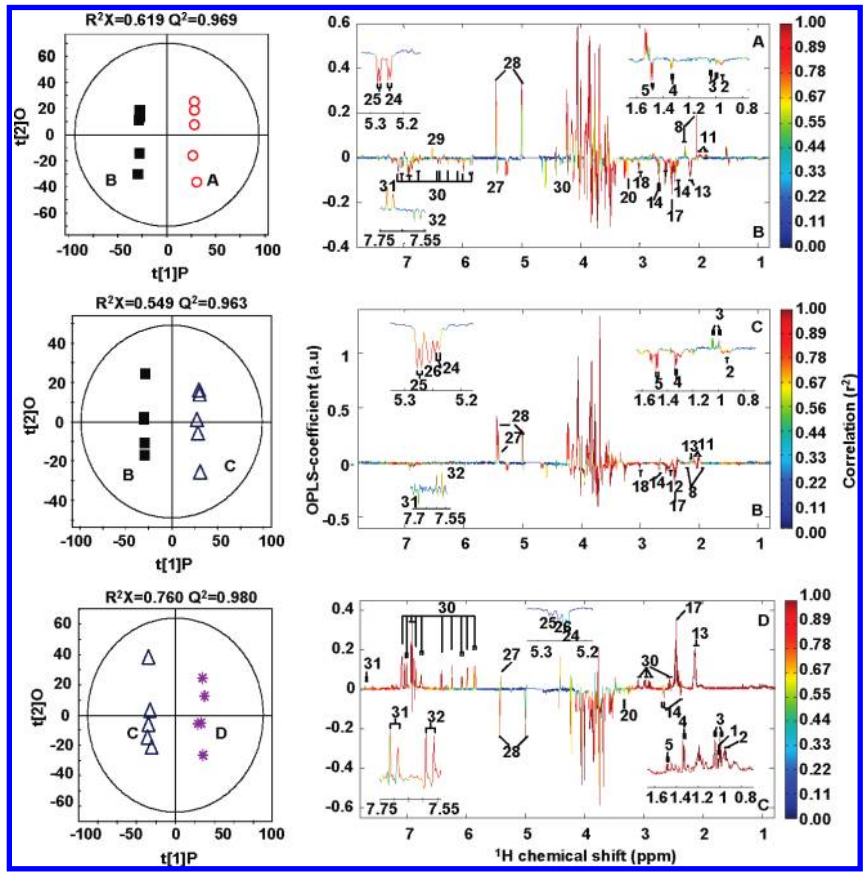

Figure 5. OPLS-DA scores (left) and coefficient-coded loadings plots (right) derived from NMR data for extracts of *Salvia miltiorrhiza* Bunge cv *Sativa* obtained from four different geographic locations: A, Zhongjiang, Sichuan (○); B, Wuhan, Hubei (■); C, Anding, Hebei (Δ); and D, Nanyang, Henan (*) (see Table 1 for metabolite identification key).

altitude and soil types. However, it is not possible at present to ascertain the relative contributions of these factors and whether such metabonomic differences have impacts on the resultant pharmacological activities of SMB. Further clinical and the pharmacology researches are clearly warranted to consider the environmental effects on the efficacy of phytomedicines. Nevertheless, these results suggest that extra care has to be taken in plant metabonomics studies to take known confounding factors into consideration and raise the huge challenging issue for the herb quality controls in terms of consistency.

To focus on the secondary metabolites, LC−DAD-MS data were also analyzed. In the case of LC−UV data, areas of 13 quantifiable peaks corresponding to 7 polyphenolic acids and 6 tanshinones were subjected to OPLS-DA. The results (Figure S5, Supporting Information) showed significant intergroup differences in the secondary metabolite composition of SMB grown at different locations. Detailed loadings and coefficient analysis revealed that compared with Zhongjiang samples (A), Wuhan SMB samples (B) contained more salvianolic acid B and rosmarinic acid but less danshensu and lithospermic acid, which was consistent with the quantification and NMR results (Table 3); Wuhan samples also contained more prolithospermic acid derivative, 15,16-dihydrotanshinone I, trijuganone B but less salvianolic acid H/I, cryptotanshinone and tanshinone IIA, all which were not detectable in NMR.

Compared with Anding samples, Wuhan SMB samples contained more lithospermic acid and less rosmarinic acid, which was in good agreement with the quantification and NMR results (Table 3); Wuhan samples also contained more danshensu and prolithospermic acid derivative but less salvianolic acids (B, H/I) and some tanshinones such as cryptotanshinone and tanshinone IIA than Anding samples. This again provided complementary information to the NMR results. Anding samples contained less rosmarinic acid, lithospermic acid and salvianolic acid B than Nanyang samples, which agreed well with the quantification and NMR results; Anding samples also contained less other polyphenolic acids including danshensu, salvianolic acid H/I, salvianolic acid L, and tanshinones such as cryptotanshinone, tanshinone IIA and two dihydrotanshinones. These LC−UV results were in reasonable agreement with the quantification and NMR results for the abundant secondary metabolites. More importantly, LC−UV results also provided information on much more secondary metabolites including both polyophenolic acids and tanshinones confirming advantages of the combined NMR and LC−UV results.

Furthermore, areas of 17 and 27 quantifiable LC−MS peaks in the negative and positive ion modes, respectively, were analyzed for SMB secondary metabolites from different locations (see Figure S6, S7 and Table S1 for details, Supporting Information). Under negative ion MS mode, OPLS-DA (Figure S7a, Supporting Information) results showed that Wuhan sample contained less lithospermic acid which was consistent with both quantification and NMR results. The results further indicated that this sample contained significantly more ferulic acid and prolithospermic acid derivative but less danshensu, caffeic acid, salvianolic acids (F, H/I and L), miltipolone and salvinal than Zhongjiang samples (A), which were not detectable in NMR. However, LC−MS results indicated that Wuhan

samples contained less salvianolic acid B with no differences for rosmarinic acid, which was not consistent with quantification and NMR results probably due to lack of linear correlation between analyte signal intensity and concentration in MS.

Compared with Anding sample, Wuhan SMB contained more lithospermic acid, ferulic acid and prolithospermic acid derivative but less rosmarinic acid, salvianolic acids (H/I, L), caffeic acid dimer, miltipolone, maslinic acid and salvinal. Although the results for lithospermic acid and rosmarinic acid agreed well with the quantification and NMR data, the results on salvianolic acid B were inconsistent with the results from NMR. Compared with Nanyang samples, the Anding SMB had statistically higher levels in caffeic acid, ferulic acid and salvianolic acid H/I and lower levels in salvianolic acid L, caffeic acid dimer, salvinal, tomentic acid, maslinic acid and miltipolone. The results for lithospermic acid were consistent with the quantification and NMR results. The levels of salvianolic acid B, rosmarinic acid and danshensu appeared to be lower in Anding samples though without statistical significance ($p > 0.05$) which was not completely agreeable with the quantification and NMR results.

In the positive ion mode, OPLS-DA (Figure S7b, Supporting Information) results showed that compared with the Zhongjiang SMB, the Wuhan SMB contained significantly higher levels in rosmarinic acid, prolithospermic acid derivative, tanshinone IIB, 15,16-dihydrotanshinone I and trijuganone B but lower levels in some polyphenolic acids (e.g., danshensu, lithospermic acid and caffeic acid), β-sitosterol and some terpenoids (e.g., cryptotanshinone and tanshinone I). Wuhan samples contained less salvianolic acid B than the Zhongjiang samples which was inconsistent with its quantity and NMR results. Compared with Anding ones (C), Wuhan SMB samples (B) contained more lithospermic acid, prolithospermic acid derivative and tanshinone IIB but less salvianolic acid H/I, caffeic acid dimer, β-sitosterol and some terpenoids (e.g., cryptotanshinone, tanshinone IIA and trijuganones). No statistical significance was found for salvianolic acid B which was consistent with their quantities in those two groups of samples and NMR results. Anding SMB contained less polyphenolic acids (e.g., rosmarinic acid and lithospermic acid), β-sitosterol and tanshinones (e.g., cryptotanshinone, tanshinone IIA and trijuganones) than the Nanyang ones. Salvianolic acid B level appeared to be lower in Anding samples though no statistical significance was found, which was yet again inconsistent with its quantity and NMR results.

The above results consistently suggest that LC−MS results are not entirely agreeable to the quantitative and NMR results although such methods have provided detections of much more secondary metabolites. This is probably due to the vastly different MS response coefficients and different sensitivity of such responses to slight variations of spectrometer conditions for different metabolites. This further suggests that when LC−MS methods are employed for metabolite profiling, *in situ* calibration is probably necessary.

Metabonomic Differences between Three *S. miltiorrhiza* Bunge Cultivars. ^{1}H NMR spectra (Figure 3) of SMB extracts from three different cultivars, namely, *S. miltiorrhiza* Bunge cv. *Sativa* (SA), *S. miltiorrhiza* Bunge cv. *Foliolum* (SF) and *S. miltiorrhiza* Bunge cv. *Silcestris* (SI), showed marked concentration differences for many metabolites although the types of metabolites were broadly similar. Raffinose (δ5.44) and succinate (δ2.42) were most abundant metabolites in these SMB cultivars with intense characteristic NMR signals whereas

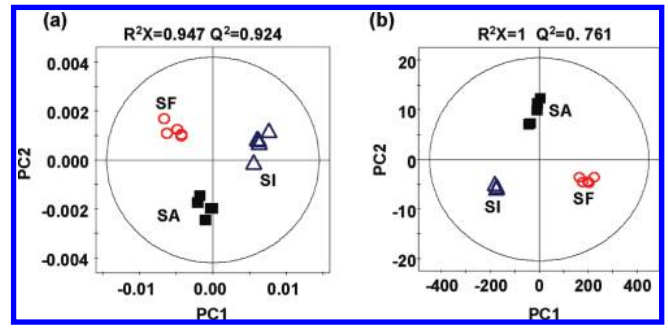

Figure 6. PCA scores plots derived respectively from (a) NMR and (b) LC−UV (280 nm) data for extracts obtained from *Salvia miltiorrhiza* Bunge cv. *Sativa* (SA, ■), cv. *Foliolum* (SF, ○) and cv. *Silcestris* (SI, △).

salvianolic acid B was the most prominent secondary metabolite. The PCA scores plots from NMR (Figure 6a) and LC−UV data (Figure 6b) showed clear separation for three cultivars and tight intragroup clustering. Such simple method will be probably useful in identifying these cultivars in terms of product quality control and perhaps authentication applications.

Comparative OPLS-DA results provided detailed information on the quantity and significance of metabolites contributing to the intercultivar differences in the forms of correlation coefficients and metabolite contents (Table 4). The coefficient-coded loadings plots (Figure 7) showed that compared with the cultivar SA, SF contained more glutamine, pyroglutamate, succinate, melibiose and salvianolic acid B but less proline and malate. SI showed higher levels in sucrose and raffinose but lower levels in some amino acids (e.g., proline and glutamine), succinate, malate, salvianolic acid B and lithospermic acid than SA. Compared with SI, SF contained more proline, glutamine, pyroglutamate, succinate, melibiose, salvianolic acid B and lithospermic acid but less malate, sucrose and raffinose. Statistical analysis results of metabolite concentrations confirmed the findings from the OPLS-DA although the latter was much more efficient especially when dealing with a large number of variables in multiple-samples. These results showed that significant metabonomic differences were present for three SMB cultivars in both primary and secondary metabolites probably resulting from the cultivation induced biological characters. This also suggests that NMR-based metabonomics approach is an importance molecular phenotying method for different ecotypes especially in subspecies levels.

To focus on the phenotypic variations of SMB in the secondary metabolism, we also analyzed the changes of 12 SMB secondary metabolites with quantifiable peaks in LC−DAD profiles including 6 polyphenolic acids and 6 tanshinones. The OPLS-DA results (Figure S8) showed that compared with SA, SF contained significantly higher levels of salvianolic acid B. SI contained more salvianolic H/I than SA together with less tanshinones (e.g., cryptotanshinone, tanshinone I and IIA) and some other polyphenolic acids (e.g., rosmarinic acid, lithospermic acid and salvianolic acid B). Compared with SI, SF had significantly lower levels in salvianolic acid H/I but higher levels in tashinones (e.g., cryptotanshinone, tanshinone I and dihydrotanshinones) and some other polyphenolic acids (e.g., danshensu and salvianolic acid L). Cultivar SF also contained more rosmarinic acid, lithospermic acid and salvianolic acid B than SI. These results on salvianolic acid B, lithospermic acid and rosmarinic acid were agreeable with NMR and quantification results although LC−UV data offered much more information on secondary metabolites.

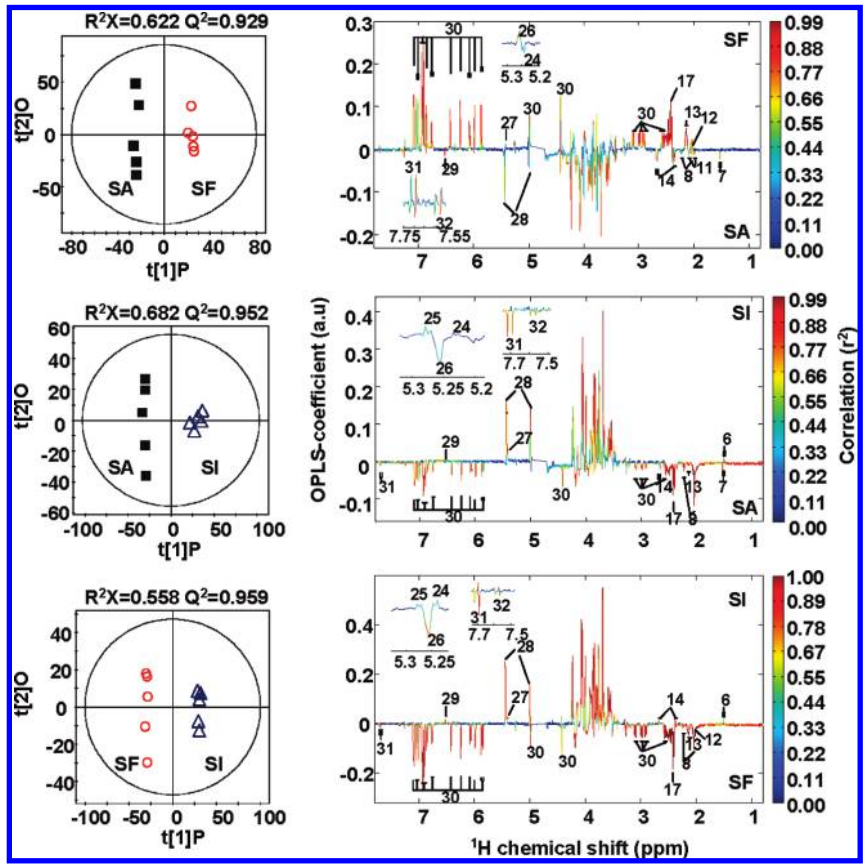

Figure 7. OPLS-DA scores (left) and coefficient-coded loadings plots (right) derived from NMR data for SMB extracts obtained from *Salvia miltiorrhiza* Bunge cv. *Sativa* (SA ■), cv. *Foliolum* (SF ○) and cv. *Silcestris* (SI Δ) (see Table 1 for metabolite identification key).

Areas of 14 and 18 quantifiable LC−MS peaks in the negative and positive ion mode, respectively, (see Figure S9, S10 and Table S1 for details, Supporting Information) were subjected to PCA and OPLS-DA. The PCA model (Figure S9, Supporting Information) of the negative and positive ion modes with two principal components showed clear separation and tight clustering for each group, confirming that three different cultivars had obviously different secondary metabolite compositions and the LC−MS methods were useful in plant ecotypic classification and phytomedicines authentication. OPLS-DA results (Figure S10, Supporting Information) showed clear differences for three SMB cultivars in terms of their secondary metabolite composition. In the negative ion mode (Figure S10a, Supporting Information), SF showed significantly higher levels in salvianolic acid B and lower levels in ferulic acid, tormentic aicd, retusin, salvinal and miltipolone than SA. Compared with SA, SI contained significant higher levels of salvianolic acid F and salvianolic acid H/I together with lower levels of tormentic acid, salvinal, miltipolone and some other polyphenolic acids (e.g., rosmarinic acid, lithospermic acid and salvianolic acid B). Compared with SI, SF contained more lithospermic acid, salvianolic acid B and L, danshensu, caffeic acid dimer and miltipolone but less salvianolic acid F and H/I, retusin and salvinal. The results on salvianolic acid B, lithospermic acid and rosmarinic acid are broadly consistent with NMR and quantification results (Table 4).

In the positive mode (Figure S10b, Supporting Information), SF showed significantly higher levels of salvianolic acid B but lower amounts of 1-ketoisocryptotanshinone, trijuganone C and cryptotanshinone than SA. Compared with both SA and SF, SI contained statistically higher levels of salvianolic acid H/I but lower levels of β-sitosterol, tashinones (e.g., cryptotanshinone, dihydrotanshinones and trijuganones) and some other polyphenolic acids (e.g., salvianolic acid B, rosmarinic acid and lithospermic acid). The results on salvianolic acid B and lithospermic acid agreed with NMR and quantification results whereas statistical significance for rosmarinic acid was not. Nevertheless, LC−DAD-MS results clearly revealed significant differences for three SMB cultivars in their secondary metabolite composition.

It has to be said that the linear correlation between signal intensity (or peak areas) and metabolite concentrations were not firmly available in LC−DAD-MS profiles of these cultivars. In SI extracts, for example, LC−UV profile (Figure S2, Supporting Information) showed that the peak-area-ratio (PAR) was 16:3:1 for salvianolic acid B, lithospermic acid and rosmarinic acid although the molar ratio for their contents was about 10:2:1. Furthermore, LC−MS results showed that the PAR for tanshione IIA and salvianolic B was 3:2 in the positive mode (Figure S4a, Supporting Information) although their molar ratio was smaller than 1:10. Such inconsistency is also highlighted in other samples. In SF extracts, for instance, the molar ratio for cryptotanshinone and salvianolic acid B was smaller than 1:10 whereas PAR for them was about 1:6 in LC−MS profile in the positive ion mode. This further implies that when LC−DAD-MS methods are employed in metabolic profiling, the simple use of peak intensities and normalization to the sum of spectrum, which are in widespread current use, may lead to misinterpretation of results and *in situ* calibration of with standards is probably a matter of necessity.

Conclusion

The combined ^{1}H NMR and LC−DAD-MS methods provided more comprehensiveness in plant metabonomic analysis by offering complementary information on both the primary and secondary metabolites. The metabolite pool of *Salvia miltiorrhiza* Bunge was largely dominated by 32 metabolites including sugars, amino acids, carboxylic acids and polyphenolic acids. LC−DAD-MS methods provided information on only secondary metabolites with detection of 40 secondary metabolites of SMB such as polyphenolic acids, diterpenoids, flavonoids and steroids. Such methods provided an excellent approach for targeted analysis of plant secondary metabolite compositions associated with growing environments and ecotypic cultivars. Our combined methods revealed that *Salvia miltiorrhiza* Bunge had markedly different metabolite composition when growing at different geographic locations and that three different SMB cultivars also showed outstanding differences in their metabolite composition including both primary and secondary metabolites. The efficiency of the OPLS-DA approach for analyzing multiple samples and multiple groups clearly offers good potentials in plant metabolic phenotyping studies. Such combined detection and multivariate data analysis methods are of important values for plant molecular phenotyping, composition-based quality control and authenticity of functional foods in addition to phytomedicines.

Abbreviations: COSY, ^{1}H−^{1}H correlated spectroscopy; TOCSY, ^{1}H−^{1}H total correlation spectroscopy; HSQC, heteronuclear single-quantum coherence; HMBC, heteronuclear multiple-bond correlation; NMR, nuclear magnetic resonance; PCA, principal component analysis; OPLS-DA, orthogonal projection to latent structure discriminant analysis; T_1, spin−lattice relaxation time; FID, free induction decay; FT, Fourier transformation.

Acknowledgment. We acknowledge the National Natural Science Foundation of China (20825520), Ministry of Agriculture of the People's Republic of China (2009ZX08012-023B), and Chinese Academy of Sciences for financial support. We also thank Dr. Hang Zhu of Wuhan Institute of Physics and Mathematics for modifying MATLAB scripts used for color-coded OPLS-DA coefficient plots, which were initially downloaded from http://www.mathworks.com/matlabcentral.

Supporting Information Available: Table S1 and Figures S1−S10. This material is available free of charge via the Internet at http://pubs.acs.org.

References

(1) Fiehn, O.; Kopka, J.; Dormann, P.; Altmann, T.; Trethewey, R. N.; Willmitzer, L. Metabolite profiling for plant functional genomics. *Nat. Biotechnol.* **2000**, *18*, 1157–1161.

(2) Bino, R. J.; Hall, R. D.; Fiehn, O.; Kopka, J.; Saito, K.; Draper, J.; Nikolau, B. J.; Mendes, P.; Roessner-Tunali, U.; Beale, M. H.; Trethewey, R. N.; Lange, B. M.; Wurtele, E. S.; Sumner, L. W. Potential of metabolomics as a functional genomics tool. *Trends Plant Sci.* **2004**, *9*, 418–425.

(3) Fiehn, O. Metabolomics - the link between genotypes and phenotypes. *Plant Mol. Biol.* **2002**, *48*, 155–171.

(4) Nicholson, J. K.; Lindon, J. C.; Holmes, E. 'Metabonomics': understanding the metabolic responses of living systems to pathophysiological stimuli *via* multivariate statistical analysis of biological NMR spectroscopic data. *Xenobiotica* **1999**, *29*, 1181–1189.

(5) Tang, H. R.; Wang, Y. L. Metabonomics: a revolution in progress. *Prog. Biochem. Biophys.* **2006**, *33*, 401–417.

(6) Raamsdonk, L. M.; Teusink, B.; Broadhurst, D.; Zhang, N. S.; Hayes, A.; Walsh, M. C.; Berden, J. A.; Brindle, K. M.; Kell, D. B.; Rowland, J. J.; Westerhoff, H. V.; van Dam, K.; Oliver, S. G. A functional genomics strategy that uses metabolome data to reveal the phenotype of silent mutations. *Nat. Biotechnol.* **2001**, *19*, 45–50.

(7) Brindle, J. T.; Antti, H.; Holmes, E.; Tranter, G.; Nicholson, J. K.; Bethell, H. W. L.; Clarke, S.; Schofield, P. M.; McKilligin, E.; Mosedale, D. E.; Grainger, D. J. Rapid and noninvasive diagnosis of the presence and severity of coronary heart disease using ^{1}H NMR-based metabonomics. *Nat. Med.* **2002**, *8*, 1439–1444.

(8) Yang, Y. X.; Li, C. L.; Nie, X.; Feng, X. S.; Chen, W. X.; Yue, Y.; Tang, H. R.; Deng, F. Metabonomic studies of human hepatocellular carcinoma using high-resolution magic-angle spinning ^{1}H NMR spectroscopy in conjunction with multivariate data analysis. *J. Proteome Res.* **2007**, *6*, 2605–2614.

(9) Wang, Y. L.; Utzinger, J.; Saric, J.; Li, J. V.; Burckhardt, J.; Dirnhofer, S.; Nicholson, J. K.; Singer, B. H.; Brun, R.; Holmes, E. Global metabolic responses of mice to *Trypanosoma brucei brucei* infection. *Proc. Natl. Acad. Sci. U.S.A.* **2008**, *105*, 6127–6132.

(10) Holmes, E.; Loo, R. L.; Stamler, J.; Bictash, M.; Yap, I. K. S.; Chan, Q.; Ebbels, T.; De Iorio, M.; Brown, I. J.; Veselkov, K. A.; Daviglus, M. L.; Kesteloot, H.; Ueshima, H.; Zhao, L. C.; Nicholson, J. K.; Elliott, P. Human metabolic phenotype diversity and its association with diet and blood pressure. *Nature* **2008**, *453*, 396–400.

(11) Holmes, E.; Loo, R. L.; Cloarec, O.; Coen, M.; Tang, H. R.; Maibaum, E.; Bruce, S.; Chan, Q.; Elliott, P.; Stamler, J.; Wilson, I. D.; Lindon, J. C.; Nicholson, J. K. Detection of urinary drug metabolite (Xenometabolome) signatures in molecular epidemiology studies via statistical total correlation (NMR) spectroscopy. *Anal. Chem.* **2007**, *79*, 2629–2640.

(12) Teague, C.; Holmes, E.; Maibaum, E.; Nicholson, J. K.; Tang, H. R.; Chan, Q. N.; Elliott, P.; Wilson, I. Ethyl glucoside in human urine following dietary exposure: detection by ^{1}H NMR spectroscopy as a result of metabonomic screening of humans. *Analyst* **2004**, *129*, 259–264.

(13) Clayton, T. A.; Lindon, J. C.; Cloarec, O.; Antti, H.; Charuel, C.; Hanton, G.; Provost, J. P.; Le Net, J. L.; Baker, D.; Walley, R. J.; Everett, J. R.; Nicholson, J. K. Pharmaco-metabonomic phenotyping and personalized drug treatment. *Nature* **2006**, *440*, 1073–1077.

(14) Yap, I. K. S.; Clayton, T. A.; Tang, H.; Everett, J. R.; Hanton, G.; Provost, J. P.; Le Net, J. L.; Charuel, C.; Lindon, J. C.; Nicholson, J. K. An integrated metabonomic approach to describe temporal metabolic disregulation induced in the rat by the model hepatotoxin allyl formate. *J. Proteome Res.* **2006**, *5*, 2675–2684.

(15) Bundy, J. G.; Lenz, E. M.; Bailey, N. J.; Gavaghan, C. L.; Svendsen, C.; Spurgeon, D.; Hankard, P. K.; Osborn, D.; Weeks, J. A.; Trauger, S. A.; Speir, P.; Sanders, I.; Lindon, J. C.; Nicholson, J. K.; Tang, H. R. Metabonomic assessment of toxicity of 4-fluoroaniline, 3,5-difluoroaniline and 2-fluoro-4-methylaniline to the earthworm *Eisenia veneta* (Rosa): Identification of new endogenous biomarkers. *Environ. Toxicol. Chem.* **2002**, *21*, 1966–1972.

(16) Ding, L. N.; Hao, F. H.; Shi, Z. M.; Wang, Y. L.; Zhang, H. X.; Tang, H. R.; Dai, J. Y. Systems biological responses to chronic perfluorododecanoic acid exposure by integrated metabonomic and transcriptomic studies. *J. Proteome Res.* **2009**, *8*, 2882–2891.

(17) Choi, Y. H.; Tapias, E. C.; Kim, H. K.; Lefeber, A. W. M.; Erkelens, C.; Verhoeven, J. T. J.; Brzin, J.; Zel, J.; Verpoorte, R. Metabolic discrimination of *Catharanthus roseus* leaves infected by phytoplasma using ^{1}H NMR spectroscopy and multivariate data analysis. *Plant Physiol.* **2004**, *135*, 2398–2410.

(18) Tikunov, Y.; Lommen, A.; de Vos, C. H. R.; Verhoeven, H. A.; Bino, R. J.; Hall, R. D.; Bovy, A. G. A novel approach for nontargeted data analysis for metabolomics. Large-scale profiling of tomato fruit volatiles. *Plant Physiol.* **2005**, *139*, 1125–1137.

(19) Roessner, U.; Luedemann, A.; Brust, D.; Fiehn, O.; Linke, T.; Willmitzer, L.; Fernie, A. R. Metabolic profiling allows comprehensive phenotyping of genetically or environmentally modified plant systems. *Plant Cell* **2001**, *13*, 11–29.

(20) Weckwerth, W.; Loureiro, M. E.; Wenzel, K.; Fiehn, O. Differential metabolic networks unravel the effects of silent plant phenotypes. *Proc. Natl. Acad. Sci. U.S.A.* **2004**, *101*, 7809–7814.

(21) Ward, J. L.; Harris, C.; Lewis, J.; Beale, M. H. Assessment of ^{1}H NMR spectroscopy and multivariate analysis as a technique for metabolite fingerprinting of *Arabidopsis thaliana*. *Phytochemistry* **2003**, *62*, 949–957.

(22) Wang, Y. L.; Tang, H. R.; Nicholson, J. K.; Hylands, P. J.; Sampson, J.; Whitcombe, I.; Stewart, C. G.; Caiger, S.; Oru, I.; Holmes, E. Metabolomic strategy for the classification and quality control of phytomedicine: A case study of chamomile flower (*Matricaria recutita* L.). *Planta Med.* **2004**, *70*, 250–255.

(23) Le Gall, G.; Colquhoun, I. J.; Defernez, M. Metabolite profiling using ^{1}H NMR spectroscopy for quality assessment of green tea, *Camellia sinensis* (L.). *J. Agric. Food Chem.* **2004**, *52*, 692–700.

(24) Biais, B.; Allwood, J. W.; Deborde, C.; Xu, Y.; Maucourt, M.; Beauvoit, B.; Dunn, W. B.; Jacob, D.; Goodacre, R.; Rolin, D.; Moing, A. ^{1}H NMR, GC-EI-TOFMS, and data set correlation for fruit metabolomics: application to spatial metabolite analysis in melon. *Anal. Chem.* **2009**, *81*, 2884–2894.
(25) Bottcher, C.; von Roepenack-Lahaye, E.; Willscher, E.; Scheel, D.; Clemens, S. Evaluation of matrix effects in metabolite profiling based on capillary liquid chromatography electrospray ionization quadrupole time-of-flight mass spectrometry. *Anal. Chem.* **2007**, *79*, 1507–1513.
(26) Xiao, C. N.; Dai, H.; Liu, H. B.; Wang, Y. L.; Tang, H. R. Revealing the metabonomic variation of rosemary extracts using ^{1}H NMR spectroscopy and multivariate data analysis. *J. Agric. Food Chem.* **2008**, *56*, 10142–10153.
(27) Dai, H.; Xiao, C. N.; Liu, H. B.; Tang, H. R. Combined NMR and LC−MS analysis reveals the metabonomic changes in *Salvia Miltiorrhiza* Bunge induced by water depletion. *J. Proteome Res.* **2010**; DOI: pr900995m.
(28) Onitsuka, M.; Fujiu, M.; Shinma, N.; Maruyama, H. B. New platelet aggregation inhibitors from Tan-Shen; radix of *Salvia Miltiorrhiza* Bunge. *Chem. Pharm. Bull.* **1983**, *31*, 1670–1675.
(29) Baillie, A. C.; Thomson, R. H. Naturally occurring quinones. Part XI. tanshinones. *J. Chem. Soc. C* **1968**, 48–52.
(30) Sugiyama, A.; Zhu, B. M.; Takahara, A.; Satoh, Y.; Hashimoto, K. Cardiac effects of *Salvia miltiorrhiza*/*Dalbergia odorifera* mixture, an intravenously applicable Chinese medicine widely used for patients with ischemic heart disease in China. *Circ. J.* **2002**, *66*, 182–184.
(31) Wasser, S.; Ho, J. M. S.; Ang, H. K.; Tan, C. E. L. *Salvia miltiorrhiza* reduces experimentally-induced hepatic fibrosis in rats. *J. Hepatol.* **1998**, *29*, 760–771.
(32) Zhang, K. Q.; Bao, Y. D.; Wu, P.; Rosen, R. T.; Ho, C. T. Antioxidative components of Tanshen (*Salvia Miltiorrhiza* Bunge). *J. Agric. Food Chem.* **1990**, *38*, 1194–1197.
(33) Chen, C.; Tang, H. R.; Sutcliffe, L. H.; Belton, P. S. Green tea polyphenols react with 1,1-diphenyl-2-picrylhydrazyl free radicals in the bilayer of liposomes: direct evidence from electron spin resonance studies. *J. Agric. Food Chem.* **2000**, *48*, 5710–5714.
(34) Zhang, X. G.; Wang, Y. M.; Luo, G. A.; Cheng, F. X. Studies on resource characteristics of *Salvia miltiorrhiza* varieties. *Chin. Tradit. Herb. Drugs* **2002**, *33*, 742–747.
(35) Djoukeng, J. D.; Arbona, V.; Argamasilla, R.; Gomez-Cadenas, A. Flavonoid profiling in leaves of *Citrus* genotypes under different environmental situations. *J. Agric. Food Chem.* **2008**, *56*, 11087–11097.
(36) Zhang, H. R.; Li, Z. M.; Gao, Z. M.; Cao, J. B. Analysis of tanshinone IIA and salvianolic acid B content from different *Salvia Miltiorrhiza* Bunge cultivars. *Lishizhen Med. Mater. Med. Res.* **2009**, *20*, 1173–1174.
(37) Ma, H. L.; Qin, M. J.; Qi, L. W.; Wu, G.; Shu, P. Improved quality evaluation of *Radix Salvia miltiorrhiza* through simultaneous quantification of seven major active components by high-performance liquid chromatography and principal component analysis. *Biomed. Chromatogr.* **2007**, *21*, 931–939.
(38) Trygg, J.; Wold, S. Orthogonal projections to latent structures (O-PLS). *J. Chemometr.* **2002**, *16*, 119–128.
(39) Fan, W. M. T. Metabolite profiling by one and two dimensional NMR analysis of complex mixtures. *Prog. Nucl. Magn. Reson. Spectrosc.* **1996**, *28*, 161–219.
(40) Sobolev, A. P.; Brosio, E.; Gianferri, R.; Segre, A. L. Metabolic profile of lettuce leaves by high-field NMR spectra. *Magn. Reson. Chem.* **2005**, *43*, 625–638.
(41) Lin, Y. L.; Wang, C. N.; Shiao, Y. J.; Liu, T. Y.; Wang, W. Y. Benzolignanoid and polyphenols from *Origanum vulgare*. *J. Chin. Chem. Soc.* **2003**, *50*, 1079–1083.
(42) Liu, A. H.; Lin, Y. H.; Yang, M.; Guo, H.; Guan, S. H.; Sun, J. H.; Guo, D. A. Development of the fingerprints for the quality of the roots of *Salvia miltiorrhiza* and its related preparations by HPLC-DAD and LC-MS^{n}. *J. Chromatogr., B* **2007**, *846*, 32–41.
(43) Tanaka, T.; Nishimura, A.; Kouno, I.; Nonaka, G.; Young, T. J. Isolation and characterization of yunnaneic acids A-D, four novel caffeic acid metabolites from *Salvia yunnanensis*. *J. Nat. Prod.* **1996**, *59*, 843–849.
(44) Mannina, L.; Patumi, M.; Proietti, N.; Bassi, D.; Segre, A. L. Geographical characterization of Italian extra virgin olive oils using high-field ^{1}H NMR spectroscopy. *J. Agric. Food Chem.* **2001**, *49*, 2687–2696.

PR901045C